

## A Keck/DEIMOS Kinematic Study of Andromeda IX: dark matter on the smallest galactic scales

Scott C. Chapman<sup>1</sup>, Rodrigo Ibata<sup>2</sup>, Geraint F. Lewis<sup>3</sup>, Annette M. N. Ferguson<sup>4</sup>, Mike Irwin<sup>5</sup>, Alan McConnachie<sup>5</sup>, Nial Tanvir<sup>6</sup>

### ABSTRACT

We present the results of a kinematic survey of the dwarf spheroidal satellite of M31, Andromeda IX, which appears to be the lowest surface brightness and also the faintest galaxy ( $M_V = -8.3$ ) found to date. Using Keck/DEIMOS spectroscopic data, we have measured its velocity relative to M31, its velocity dispersion, and its metallicity. It exhibits a significant velocity dispersion  $\sigma_v = 6.8_{-2.0}^{+3.0} \text{ km s}^{-1}$ , which coupled with the low luminosity implies a very high mass to  $V$ -band light ratio,  $M/L \sim 93_{-50}^{+120} M_\odot/L_\odot$  ( $M/L > 17 M_\odot/L_\odot$  at 99% confidence). Unless strong tidal forces have perturbed this system, this smallest of galaxies is a highly dark matter dominated system.

*Subject headings:* galaxies: dwarf — galaxies: individual (Andromeda V) — galaxies: individual (Andromeda IX) — galaxies: evolution — Local Group

### 1. Introduction

Hierarchical structure formation models, such as  $\Lambda$ CDM, predict that large spiral galaxies like the Milky Way (MW) or Andromeda (M31) arise from successive mergers of small

---

<sup>1</sup>California Institute of Technology, Pasadena, CA 91125; [schapman@astro.caltech.edu](mailto:schapman@astro.caltech.edu)

<sup>2</sup> Observatoire de Strasbourg, 11, rue de l'Université, F-67000, Strasbourg, France

<sup>3</sup> Institute of Astronomy, School of Physics, A29, University of Sydney, NSW 2006, Australia

<sup>4</sup>Institute for Astronomy, University of Edinburgh, Royal Observatory, Blackford Hill, Edinburgh, EH9 3HJ, U.K.

<sup>5</sup> Institute of Astronomy, Madingley Road, Cambridge, CB3 0HA, U.K.

<sup>6</sup> Centre for Astrophysics Research, Univ. of Hertfordshire, Hatfield, AL10 9AB, UK

galaxies and from the smooth accretion of gas. At late times, when a dominant central mass is in place, the main mode of mass acquisition is via the cannibalization of low mass satellites which fall into the gravitational potential well of the massive host.

These  $\Lambda$ CDM models are highly successful at explaining observations on large scales. However, the models predict an overabundance of low-mass dark subhalos, which is inconsistent by 1–2 orders of magnitude with the number of observed dwarf galaxies (Klypin et al. 1999; Moore et al. 1999; Benson et al. 2002a). Large uncertainties remain on the level of disagreement between model and observation because of the difficulty in constraining the faint end of the galaxy luminosity function; the low surface brightnesses expected for the faintest galaxies ( $\mu_V \gtrsim 26 \text{ mag arcsec}^{-2}$ ; e.g., Caldwell 1999; Benson et al. 2002b) imply that ground-based surveys are likely incomplete even in nearby galaxy groups. From a theoretical perspective, star formation in low mass subsystems would have to be suppressed (e.g., photoionization in the early universe) to bring models and observations into closer accord. The result of this hydro-dynamical modification would be a shallower faint-end slope for the  $z \sim 0$  galaxy luminosity function (e.g., Somerville 2002; Benson et al. 2002b; Willman et al. 2004). A critical prediction of this solution is that dwarf galaxies should then be embedded in much larger, more massive dark subhalos (Stoehr et al. 2002).

Observational progress can be made in the case of the Local Group (LG), where galaxies can be resolved into stars, thereby probing much fainter effective surface brightness limits (Ibata et al. 2001; Ferguson et al. 2002; Lewis et al. 2004; Willman et al. 2005). Several recent and ongoing surveys are yielding exciting detections of low surface brightness features and new dwarf galaxy candidates around our nearest giant neighbour, M31 (e.g. Ibata et al. 2001; Ferguson et al. 2002; Zucker et al. 2004a,b; McConnachie et al. 2004). Of particular interest is the system And IX, which was first reported by the Sloan Digital Sky Survey team (Zucker et al. 2004a), and is readily visible in previously-published maps from the M31 INT Wide-Field Camera Survey (Ferguson et al. 2002). Andromeda IX is unique in that it is the lowest surface brightness galaxy found to date ( $\mu_{V,0} \sim 26.8 \text{ mag arcsec}^{-2}$ ), and at the distance estimated from the position of the tip of the red giant branch ( $I = 20.50 \pm 0.03$ ,  $M_I^{TRGB} = 4.065$ ,  $(m - M)_0 \sim 24.42$ ) of  $765 \pm 24 \text{ pc}$  (McConnachie et al. 2005a), Andromeda IX would also be the faintest galaxy known ( $M_V = -8.3$ ). It is therefore an extremely important target for further study, with the potential to place strong constraints on both the LG luminosity function and the physics of galaxy formation at the smallest scales. In this letter, we present the results of a kinematic survey of the Andromeda IX dwarf spheroidal satellite of M31. We have assumed for this paper a distance to M31 of  $785 \pm 25 \text{ kpc}$  ( $(m - M)_0 = 24.47 \pm 0.07$ ; (McConnachie et al. 2005a)).

## 2. Properties of Andromeda IX

Andromeda IX reveals itself in the INT WFC survey data as an enhancement of metal poor RGB stars at a location of  $1.8^\circ$  to the E and  $1.9^\circ$  to the N of the nucleus of M31. Figure 1 shows a color-magnitude diagram (CMD) centered on Andromeda IX and a nearby comparison region of equivalent area. The excess red giant branch (RGB) stars on the blueward side of the general M31 RGB locus form a well-defined Andromeda IX locus with an apparent RGB tip at  $I = 20.5$  consistent with the distance of M31, and if representative of an old stellar population,  $[Fe/H] \sim -1.5$  (McConnachie et al. 2005a). This metallicity value could be a slight overestimate given the presence of contaminating stars from the halo of M31; indeed the deeper study by Harbeck et al. (2005) found that the Andromeda IX population is more metal-poor ( $[Fe/H] \sim -2.0$ ).

Although sparsely populated, the radial profile, computed as the median counts in circular annuli centered on  $00^h52^m52^s + 43^\circ12'00''$ , is well defined and is shown background-corrected in the right-hand panel of Figure 2. Exponential and Plummer-law profiles provide adequate fits, with the scale radius from the exponential fit being  $r_s = 1.4 \pm 0.3'$  (corresponding to  $r_s = 315 \pm 65$  pc; half-light radius  $r_h = 530 \pm 110$  pc), a value comparable to the other Andromedan dSph companions (Mateo 1998; Caldwell 1999; McConnachie & Irwin 2005b). The error estimates include the uncertainty in the background subtraction.

The luminosity of the dwarf galaxy is constrained by measuring the integrated flux, or surface brightness, distribution. The processing procedure (Irwin et al. 2004) is relatively straightforward: first the existing derived object catalogues are used to define a “bright” foreground star component, one magnitude above the RGB tip (to allow for potential AGB stars); a circular aperture is excised around each foreground star and the flux within set to the local sky level interpolated from a whole-frame background map (the size of the aperture is the maximum of 4 times the catalog-recorded area at the detection isophote or a diameter 4 times the derived FWHM seeing); each frame is then rebinned on a  $3 \times 3$  grid to effectively create  $1''$  pixels; the binned image is then further smoothed using a 2D Gaussian filter of FWHM  $5''$ .

The result of this is to produce a coarsely-sampled smooth image containing both the resolved and unresolved light contribution from the dwarf. Elliptical apertures centered on the dwarf are then placed over the mosaic. The background is determined by robustly fitting a smoothly-varying surface over the whole mosaic area. The central surface brightness can then be trivially measured by deriving the radial profile, defined as the background-corrected median flux value within elliptical annuli. The variation in the flux from the multiple background measures gives a good indication of the flux error, which is, of course, dominated by systematic fluctuations rather than by random noise. Since the systematics are

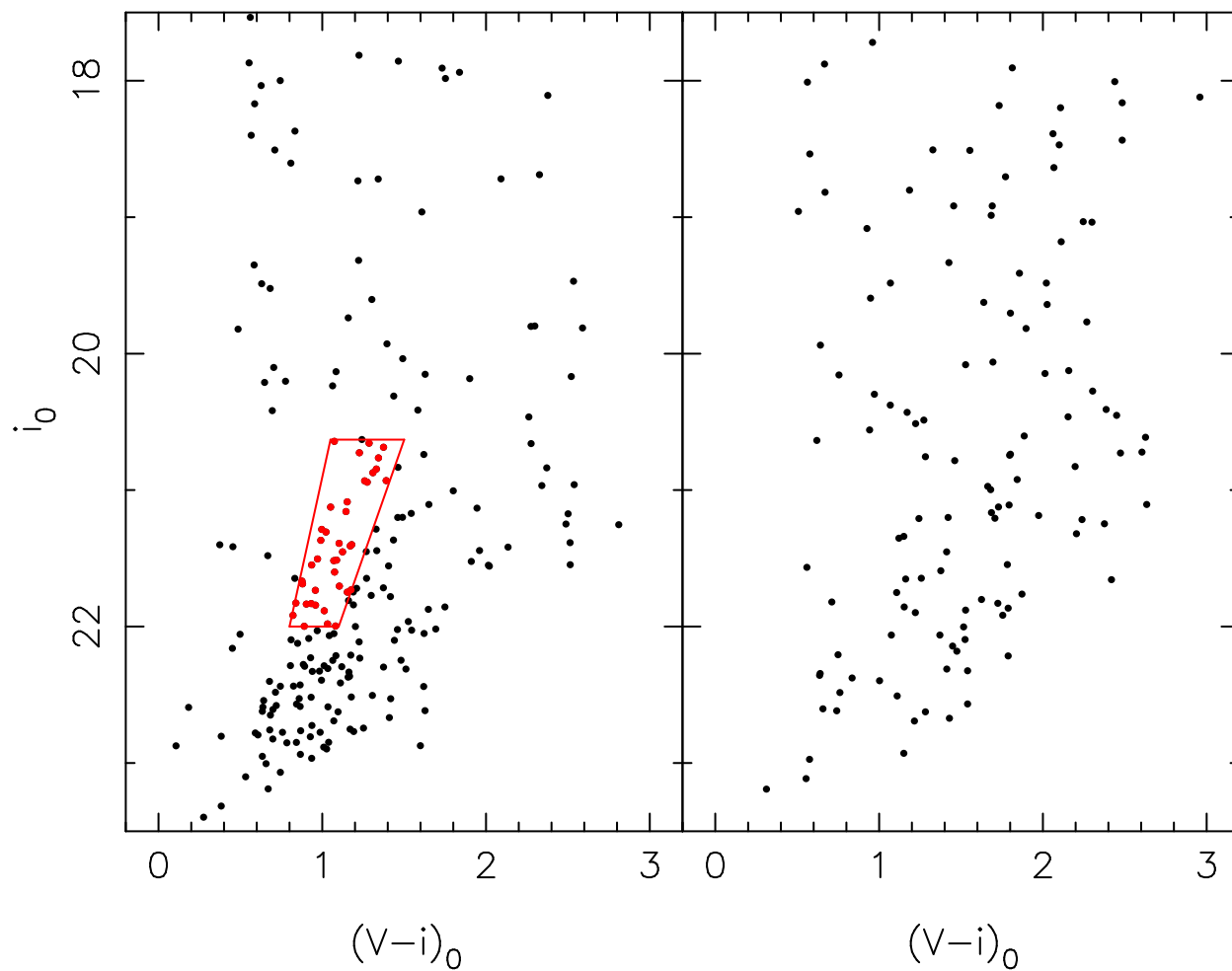


Fig. 1.— Left panel: the color-magnitude diagram from a region centered on Andromeda IX with radius  $2.5'$ . The quadrilateral shows the adopted CMD selection box, designed to select Andromeda IX RGB stars, which are blue and metal-poor, for spectroscopic follow-up. Right panel: a comparison region of the same size  $10'$  to the North.

dominated by random residual foreground star halos and scattered light from bright stars, possibly just outside the field-of-view, we chose to mitigate the effect by defining the size of the elliptical aperture to be equivalent to the geometric half-light radius derived from the number density profile. The estimated total flux is then scaled to allow for this correction. In this way we derive  $M_V = -8.3 \pm 0.2$  (corrected for extinction), in agreement with the estimate of  $M_V = -8.3$  from Zucker et al. (2004a); and measure a central surface brightness  $\Sigma_V = 26.5 \pm 0.3 \text{ mag arcsec}^{-2}$ .

### 3. Spectroscopic Observations and Data Analysis

Spectra for Andromeda IX were obtained with the DEIMOS spectrograph on the Keck2 telescope on the night of Sept. 13, 2004, under photometric conditions and seeing from  $0.5''$ – $0.8''$ . We employed the 1200 l/mm grating covering the wavelength range 6400–9000Å, with a spectral resolution of  $\sim 1.5\text{Å}$ . The observations pioneered a new approach with DEIMOS: using a ‘fibre-hole’  $0.7''$  slitlet approach packing  $\sim 600$  holes per mask.

For the Andromeda IX field, we constructed a ‘fibre-hole’ mask with 623 holes assigned within the  $16' \times 5'$  DEIMOS field. This ‘fibre-hole’ approach adopted in Sept. 2004 proved to be very successful, giving Poisson-limited sky-subtraction (down to  $i = 21.5$ ) by assigning holes to monitor the sky spectrum. Stars were selected for observation primarily within a color-magnitude box designed to choose red-giant branch stars from the  $5'$  region surrounding Andromeda IX. This color-magnitude selection box is displayed in Figure 1. We then let the DEIMOS configuration program randomly choose objects as fillers with I-band magnitudes between  $20.5 < I < 22.0$  and colors  $1.0 < V - i < 4.0$ . Both metal-poor and metal-rich populations will be present in this selection. The fiber-hole diameters were milled at  $0.7''$  to match the median seeing. A total of 289 stars and 334 sky slits were assigned in this low-density field in the M31 outer halo.

The Andromeda IX mask was observed for three integrations of 20 min each, nodding to blank sky for 5 min between each exposure to ensure that an adequate sky model could be constructed. The spectroscopic images were processed and combined using the pipeline software developed by our group. This software debiases, performs a flat-field, extracts, wavelength-calibrates and sky-subtracts the spectra. The radial velocities of the stars were then measured with respect to a Gaussian model of the CaII triplet lines (similar to the technique of Wilkinson et al. (2004)). By fitting the three Ca triplet lines separately, an estimate of the radial velocity accuracy was obtained for each radial velocity measurement. The measurements have typical uncertainties of  $5 \text{ km s}^{-1}$  to  $10 \text{ km s}^{-1}$ . A sample of 138 stars yielded a continuum  $S/N > 10$  and cross-correlations with velocity uncertainties of less than

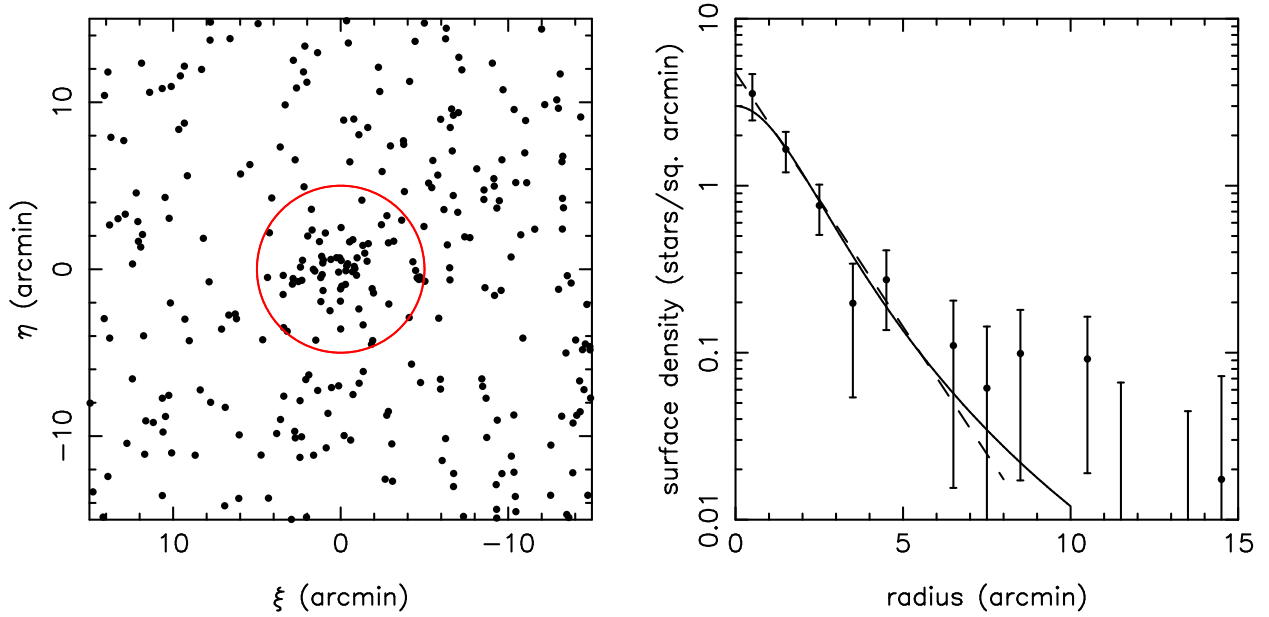


Fig. 2.— The left panel shows the positions of the stars in a  $15 \times 15'$  region around the center of Andromeda IX that fall in the RGB selection box of Figure 1. The  $5'$  radius circle used for selecting radial velocity members is also displayed. The right-hand panel shows the surface density profile of these RGB stars with a background component removed. This background was modelled with a sloping component that is a function of the radial distance to the center of M31; at the position of Andromeda IX the background has a number density of  $0.26 \pm 0.08 \text{ arcmin}^{-2}$ . The overlaid profiles are a Plummer model (solid line) with central density  $3.0 \text{ arcmin}^{-2}$  and scale size  $2.6'$  and an exponential profile (dashed line) with central density  $4.8 \text{ arcmin}^{-2}$  and scale size  $1.4'$ .

$15 \text{ km s}^{-1}$ , and we include only these stars in the subsequent analysis; 18 of these 138 stars lie in the Andromeda IX color selection window.

The measured radial velocities in the Andromeda IX field are shown in Figure 3 as a function of radial distance from the galaxy, where filled circles show the color-selected stars, while open circles are stars outside the CMD selection box. A strong foreground Galactic component is present at heliocentric velocities  $v > -150 \text{ km s}^{-1}$ , though as we show in a companion paper (Ibata et al. 2005), below this velocity the Galactic contamination is small. Close to the center of Andromeda IX there is a small but clear kinematic grouping of stars which also lie on the Andromeda IX RGB. We first define an inner sample to be the 5 stars observed within a radius of one exponential scale-length ( $1.4'$ ); this sample has mean of  $v = -210.1 \text{ km s}^{-1}$  and an r.m.s. dispersion of  $\sigma_v = 5.2 \text{ km s}^{-1}$ , which is tiny compared to the huge velocity spread of stars beyond  $5'$ , indicating that the sample is highly unlikely to be contaminated. Indeed, outside of a radius of  $5'$  not a single RGB-selected star is found within  $80 \text{ km s}^{-1}$  of this mean.

An inspection of Figure 3 shows that all stars within the RGB selection box in a radius of  $5'$  have radial velocities close to the mean of the inner sample. A fit of a maximum-likelihood Gaussian model given these data (and their uncertainties), is shown on the left-hand panel of Figure 4 (thin black lines), where we display the likelihood contours as a function of mean velocity and velocity dispersion. The most likely values are  $v = -219 \pm 4 \text{ km s}^{-1}$  and  $\sigma_v = 12.9_{-2}^{+4} \text{ km s}^{-1}$ . However, a single star at  $1.9'$  stands out in this sample of 11 objects as it is offset by  $-44.6 \text{ km s}^{-1}$  from the mean velocity of the inner sample. Since this object is potentially a contaminant, it is important to make an estimate of the expected contribution from M31 in the larger  $5'$  sample. We find that the halo in our kinematic survey of M31, as seen through windows not affected by the M31 disk or by Galactic stars (Chapman et al. 2005), can be approximated to first order with a Gaussian distribution of dispersion  $99 \text{ km s}^{-1}$ , centered at a mean velocity of  $-300 \text{ km s}^{-1}$ . We use the RGB-selected stars at radii larger than  $5'$  and with velocities  $v < -300 \text{ km s}^{-1}$  (there are two such stars) to normalise this simple halo model in the present field. A crude estimate of the expected contamination within a velocity interval of  $\pm 44.6 \text{ km s}^{-1}$  of the mean velocity of the inner sample can then be made. In this way we estimate that  $\approx 0.2$  stars contaminate the sample within  $5'$ , though the uncertainties on this estimate are clearly very large.

There is therefore some grounds to reject the velocity outlier at  $1.9'$ . Rejecting that star in the maximum-likelihood Gaussian fit results in the thick-lined likelihood contours shown in Figure 4; the fit has a mean velocity and velocity dispersion of  $v = -216 \pm 3 \text{ km s}^{-1}$  and  $\sigma_v = 6.8_{-2.0}^{+3.0} \text{ km s}^{-1}$ , respectively. The lower panel of Figure 3 shows the maximum-likelihood velocity dispersion measures, starting at the radius of the inner  $1.4'$  sample, and moving

outwards to  $5'$  adding one datum at a time. For the case of the thick-lined distribution we have rejected the velocity outlier at  $1.9'$ . Evidently, the first 5 velocity data are consistent with being drawn from a population with zero intrinsic velocity dispersion, though beyond  $1.6'$  the dispersion appears to increase to  $\sim 7 \text{ km s}^{-1}$ . We note in passing that the present dataset shows no clear radial velocity gradient. The (maximum-likelihood fitted) mean velocity of the 5 inner stars within  $1.4'$  is  $-210.6 \pm 3 \text{ km s}^{-1}$ , while the mean velocity of the sample of 5 stars between  $1.4'$  and  $5'$  (with the outlier rejected) is  $-220.4 \pm 4 \text{ km s}^{-1}$ , so the velocity difference between the two samples is less than  $2\sigma$ .

The spectra also allow a measurement of the metallicity of the dwarf galaxy using the CaT equivalent width (EW) technique. While the S/N of individual stars are typically too low to yield useful estimates of the CaT EWs, we proceeded to measure the average metallicity by stacking the RGB star spectra of the 5 highest S/N stars of our sample of 10 stars within  $r < 5'$ . We follow as closely as possible the method of Rutledge, Hesser & Stetson (1997), fitting Moffat functions to the CaII lines. The average spectrum yields a measurement of the CaT equivalent width used to estimate the metallicity as  $[Fe/H] = -2.66 + 0.42[\Sigma Ca - 0.64(V_{HB} - V_{ave})]$ , with  $\Sigma Ca = 0.5EW_{\lambda 8498} + 1.0EW_{\lambda 8542} + 0.6EW_{\lambda 8662}$ ,  $V_{HB}$  being a surface gravity correction relative to the  $V$  magnitude of the horizontal branch, and  $V_{ave} = 22.4 \pm 0.3$  the average magnitude of the Andromeda IX stars. We correct the value of  $V_{HB} = 25.17$  for M31, measured by Holland et al. (1996), by  $-0.06$  mags to account for the difference in line of sight distance between M31 and Andromeda IX. We find  $[Fe/H] = -1.5$  (on the Carretta & Gratton 1997 scale), with a large uncertainty of  $\sim 0.3$  mags which is due primarily to sky-subtraction residuals making it difficult to define the continuum level of the spectrum. This metallicity estimate confirms the previous photometric estimates of  $[Fe/H] \sim -1.5$  by McConnachie et al. (2005a) and of  $[Fe/H] \sim -2$  by Harbeck et al. (2005). A metallicity of  $[Fe/H] \sim -2$  would be closer to what we would expect for such a faint dSph, however if the mass were as large as suggested by the upper range of our kinematic analysis, a metallicity of  $[Fe/H] \sim -1.5$  would be reasonable.

#### 4. A Cold, Dark Matter dominated Accreted Companion to M31?

The mean radial velocity that we measure ( $v = -216 \pm 3 \text{ km s}^{-1}$ ) implies that Andromeda IX is almost certainly a bound satellite to M31. The relative radial velocity from M31 is then only ( $\Delta v = 84 \pm 3 \text{ km s}^{-1}$ ), while its separation from the M31 center is only  $\sim 50$  kpc. In the model of Ibata et al. (2004), the escape velocity from 50 kpc is  $550 \text{ km s}^{-1}$ ; if the velocity vector of Andromeda IX is uncorrelated with the direction vector to the observer, the chances of measuring a line of sight component of only  $84 \text{ km s}^{-1}$  if Andromeda IX is



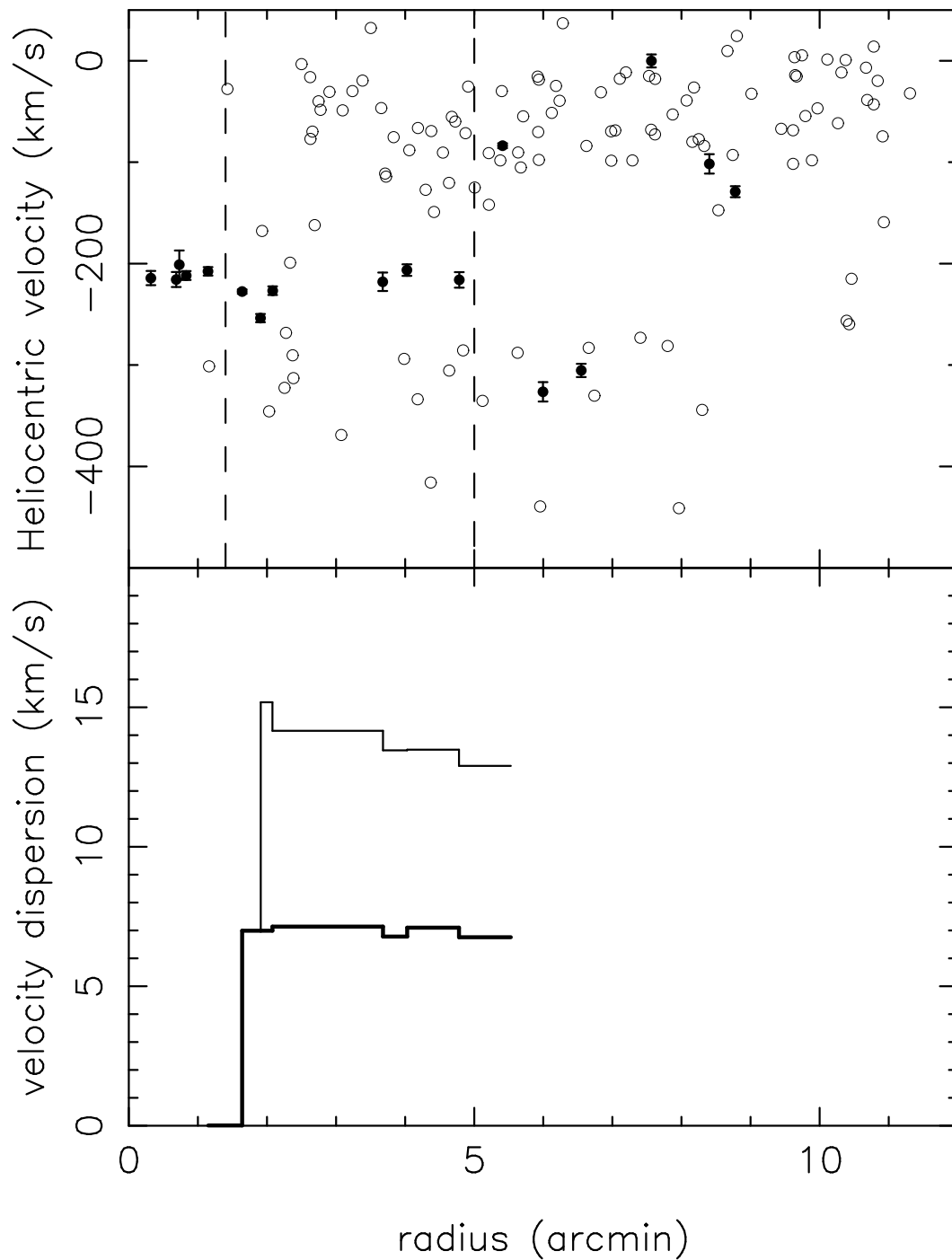


Fig. 3.— Upper panel: the radial velocities of all stars with velocity uncertainty  $< 15 \text{ km s}^{-1}$  from the 'fiber-hole' mask centered on Andromeda IX. Solid circles mark the data for the stars in the color-magnitude selection box of Figure 2; open circles are other targets. The dashed lines indicate the radial selection limits discussed in the text. The lower panel shows the derived maximum-likelihood velocity dispersion as a function of radius; the thin-line corresponds to all the data, while the thick line rejects one velocity outlier situated at  $1.9'$ .

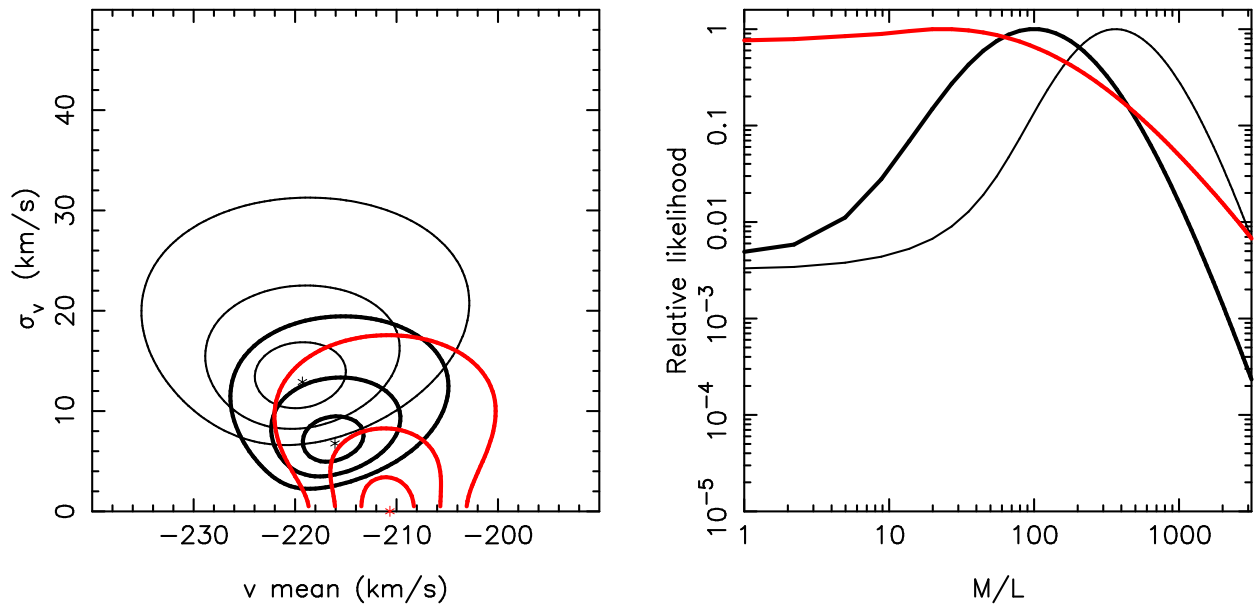


Fig. 4.— The left-hand panel shows the likelihood contours (at  $1\sigma$ ,  $2\sigma$ ,  $3\sigma$  intervals) of the mean and dispersion of the Andromeda IX population, based on radial velocity data within  $5.0'$  (black curves) and  $1.4'$  (red curves). The thick black curves show the effect of rejecting a single datum at  $r = 1.9'$ . The corresponding relative likelihood of different mass to light ratios are displayed on the right-hand panel. The thin black line is determined from the sample of 11 stars with  $r < 5'$ , while for the thick black line a single star has been rejected. The red line shows the result for the  $r < 1.4'$  sample.

unbound would be  $< 1\%$  (although uncertainty in the line of sight distance could slightly increase the probability). Andromeda IX is therefore most likely bound to M31.

The measured velocity dispersion also allows us to constrain the dark matter content of the small galaxy, if we assume virial equilibrium. The mass to light ratio of a simple spherically symmetric stellar system of central surface brightness  $\Sigma_0$ , half brightness radius  $r_{hb}$ , and central velocity dispersion  $\sigma_0$  can be estimated as:

$$M/L = \eta \frac{9}{2\pi G} \frac{\sigma^2}{\Sigma_0 r_{hb}} \quad (1)$$

Richstone & Tremaine (1986), where  $\eta$  is a dimensionless parameter which has a value close to unity for many structural models.

For our sample of stars within  $5'$ , the measured velocity dispersion is not necessarily representative of the central value of  $\sigma_0$ . However, for most models of bound stellar systems like those assumed in the core-fitting method, the velocity dispersion decreases with distance, so that our measured dispersion will be an underestimate of  $\sigma_0$  if Andromeda IX conforms to these models. Assuming that  $\sigma_v = \sigma_0$ , we show the relative likelihood of  $M/L$  values for our sample selections on the right-hand panel of Figure 4, where we have folded in the uncertainties in the half-light radius, the velocity dispersion and the central surface brightness. For the  $5'$  sample with the rejected velocity outlier, we find that the measured kinematics imply that Andromeda IX has a mass to light ratio  $M/L = 93_{-50}^{+120} M_\odot / L_\odot$  (thick black line). In particular, with this sample we can reject the possibility that Andromeda IX has  $M/L < 17 M_\odot / L_\odot$  with 99% confidence. However, this measurement depends very sensitively on our adopted sample; if we do not reject the single most discrepant velocity datum we find a higher preferred  $M/L$  value (thin black line), while if we choose the inner 5 stars alone (red lines), the mass can be consistent with zero.

The spectroscopic data we have presented here have allowed us to make a preliminary assessment of the mass and nature of this intriguing dwarf galaxy. While Andromeda IX appears to be the lowest surface brightness galaxy found to date (Zucker et al. 2004a), and also the faintest galaxy known, our preferred mass estimate ( $\sim 1.6 \times 10^7 M_\odot$ ) implies a substantial dark matter component with a mass-to-light ratio  $\sim 93$ . For comparison, applying the same procedure above to the case of the Draco dSph, the most dark matter dominated of the Milky Way satellites, which has  $\sigma_0 = 8.5 \text{ km s}^{-1}$  (Kleyna et al. 2002),  $r_{hb} = 120 \text{ pc}$  and  $\Sigma_0 = 2.2 M_\odot / \text{pc}^2$  (Irwin & Hatzidimitriou 1995) gives  $M/L = 91$  (though more detailed dynamical modelling suggests  $M/L = 440 \pm 240 M_\odot / L_\odot$  - Kleyna et al. 2002). We point out that this analysis assumes a Gaussian distribution, while there are probably too few Andromeda IX data points to support this assumption.

Although we cannot rule out the possibility that tidal effects have enhanced the extent

and velocity dispersion of this satellite, yielding a misleadingly high mass to light ratio estimate, Andromeda IX appears to be a highly dark matter dominated dSph. It therefore presents an intriguing possibility for hierarchical cold dark matter models of structure formation – that many dark matter dominated dSphs, fainter even than Andromeda IX, and lying just below the limits of detectability, may be present in the halos of giant galaxies like M31, bringing models (e.g., Moore et al. 1999; Benson et al. 2002b) into better accord with data. Nevertheless, given the small size of our sample of stars further accurate kinematic data are needed to confirm the velocity dispersion measurement, while deep photometry will help ascertain the extent to which tidal forces may be perturbing the system.

We would like to thank the referee, Steve Majewski, for his thorough comments on the manuscript which helped improve the paper. SCC acknowledges support from NASA. GFL acknowledges support through ARC DP 0343508. The research of AMNF has been supported by a Marie Curie Fellowship of the European Community under contract number HPMF-CT-2002-01758.

## REFERENCES

- Abadi, M., Navarro, J. F., Steinmetz, M., Eke, V. 2003, *ApJ*, 597, 21
- Benson, A. J., Lacey, C. G., Baugh, C. M., Cole, S., & Frenk, C. S. 2002a, *MNRAS*, 333, 156
- Benson, A. J., Frenk, C. S., Lacey, C. G., Baugh, C. M., & Cole, S. 2002b, *MNRAS*, 333, 177
- Caldwell, N. 1999, *AJ*, 118, 1230
- Carretta, E., Gratton, R. 1997, *A&AS* 121, 95
- Chapman, S. C., Ibata, R., Ferguson A. M. N., Irwin M., Lewis G., Tanvir N., 2005, in prep.
- Ferguson, A. M. N., Irwin, M. J., Ibata, R. A., Lewis, G. F., & Tanvir, N. R. 2002, *AJ*, 124, 1452
- Harbeck, D., Gallagher, J., Grebel, E., Kock, A., Zucker, D. 2005, *astro-ph/0501439*
- Holland, S., Fahlman, G. G., Richer, H. B., 1996, *AJ*, 112, 1035
- Ibata R., Irwin M., Lewis G., Ferguson A. M. N., Tanvir N., 2001, *Nature*, 412, 49.

- Ibata, R., Chapman, S. C., Irwin M., Lewis G., Ferguson A. M. N., McConnachie, A., Tanvir N., 2004, MNRAS, 351, 117
- Ibata, R., Chapman, S. C., Ferguson A. M. N., Lewis G., Irwin M., Tanvir N., 2005, astro-ph/0504164
- Irwin, M., Lewis, J., Hodgkin, S., Bunclark, P., Evans, D., McMahon, R., Emerson, J., Stewart, M., Beard, S. 2004, SPIE, 5493, 411
- Irwin, M., Hatzidimitriou, D. 1995, MNRAS 277, 1354
- Kleyna, J., Wilkinson, M., Evans, N., Gilmore, G., Frayn, C. 2002, MNRAS 330, 792
- Klypin, A., Kravtsov, A. V., Valenzuela, O., & Prada, F. 1999, ApJ, 522, 82
- Lewis, G., Ibata, R., Chapman, S., Ferguson, A, McConnachie, A., Irwin, M., Tanvir, N., 2004, PASA, 21, 203
- Mateo, M. 1998, ARA&A 36, 435
- McConnachie, A., Irwin, M., Ibata, R., Lewis, G., Chapman, S., Ferguson, A., Tanvir, N, 2004, MNRAS, astro-ph/0406055
- McConnachie, A., Irwin, M., Ibata, R., Lewis, G. Ferguson, A., Tanvir, N, 2005a, MNRAS, astro-ph/0410489
- McConnachie, A., Irwin, M., 2005b, MNRAS, submitted
- Moore, B., Ghigna, S., Governato, F., Lake, G., Quinn, T., Stadel, J., & Tozzi, P. 1999, ApJ, 524, 19
- Richstone, D. O., Tremaine, S. 1986, AJ 92, 72
- Rutledge, G., Hesser, J., Stetson, P. 1997, PASP 109, 883
- Somerville, R. S. 2002, ApJ, 572, L23
- Stoehr, F., White, S., Tormen, G., & Springel, V. 2002, MNRAS, 335, L84
- Wilkinson, M., Kleyna, J., Evans, N., Gilmore, G., Irwin, M., Grebel, E. 2004, ApJ 611, 21
- Willman, B. et al., 2005, ApJL, in press, astro-ph/0503552
- Willman, B. et al., 2004, MNRAS, 353, 639

Zucker, D. B., et al. 2004, ApJ, 612, L121

Zucker, D. B., et al., 2004, ApJ, 612, 117